Supplementary Information of

Comprehensive simulations of new particle formation events in Beijing with a cluster dynamics-multicomponent sectional model

Chenxi Li[1], Yuyang Li[2], Xiaoxiao Li[2], Runlong Cai[3], Yaxin Fan[1], Xiaohui Qiao[2], Rujing Yin[2], Chao Yan[4,5], Yishuo Guo[5], Yongchun Liu[5], Jun Zheng[6], Veli-Matti Kerminen[3], Markku Kulmala[3,5], Huayun Xiao[1]*, Jingkun Jiang[2]*

[1]School of Environmental Science and Engineering, Shanghai Jiao Tong University, 200240, Shanghai, China

[2]State Key Joint Laboratory of Environment Simulation and Pollution Control, School of Environment, Tsinghua University, 100084 Beijing, China

[3]Institute for Atmospheric and Earth System Research / Physics, Faculty of Science, University of Helsinki, 00014 Helsinki, Finland

[4]Joint International Research Laboratory of Atmospheric and Earth System Sciences, School of Atmospheric Sciences, Nanjing University, Nanjing 210023

[5]Aerosol and Haze Laboratory, Beijing Advanced Innovation Center for Soft Matter Science and Engineering, Beijing University of Chemical Technology, 100029 Beijing, China

[6]Collaborative Innovation Center of Atmospheric Environment and Equipment Technology, Nanjing University of Information Science & Technology, Nanjing, 210044, China

Correspondence to: Huayun Xiao (xiaohuayun@sjtu.edu.cn), Jingkun Jiang (jiangjk@tsinghua.edu.cn)

Information available:

S1. Calculation method of particle formation rates and survival probability

The particle formation rate $J_{d_{min}}$ defined at a particle diameter d_{min} is calculated with the following equation,

$$J_{d_{min}}(t) = \frac{\sum_{d_{min}\le d_i\le d_{max}} N_i(t+\Delta t) - \sum_{d_{min}\le d_i\le d_{max}} N_i(t)}{\Delta t} + \frac{1}{2}\sum_{d_{min}\le d_i, d_j\le d_{max}} P_{ij}\beta_{ij}N_i(t)N_j(t) + GR_{d_{max}}n_{d_{max}} + \sum_{d_{min}\le d_i\le d_{max}} CoagS_i(t)N_i(t). \quad \text{(S1)}$$

In Eq. S1, d_{max} is the upper boundary of the variable simulation domain (see section 2.2 in the main text), d_i is the particle diameter in the ith size bin, $N_i(t)$ is the particle number concentration in the ith bin, β_{ij} is the collision rate coefficient between particles in the ith and jth bin, $GR_{d_{max}}$ is the growth rate of particles with a diameter of d_{max}, $n_{d_{max}}$ is the number based particle size distribution function (in the form of dN/ddp) at d_{max}, $CoagS_i(t)$ is the coagulation loss rate for particles in the ith bin, P_{ij} takes a value of 1 if the coalesced particle is within the simulation domain and takes a value of 2 if the coalesced particle is outside the domain. Since we have chosen the simulation domain boundary to separate particles generated by NPF from preexisting particles, $n_{d_{max}}$ is small and the term $GR_{d_{max}}n_{d_{max}}$ is set to zero in the calculations.

It should be noted that Eq. S1 combines the particle flux past d_{min} from both particle growth and coagulation. Since the particle concentration in Beijing is higher than those observed in cleaner environments, including particle coagulation in formation rate calculations is necessary. Equation S1 does not account for emission of primary particles. In the presence of primary particle emissions, the first term on the right-hand side of Eq. S1 will be higher than expected if only particle growth, coagulation and loss to coagulation sinks are considered. Consequently, Eq. S1 gives a higher value of $J_{d_{min}}$ when it is applied to the observed PSD in the presence of primary particle emissions.

The survival probability $P_{d_1-d_2}$ as particles grow from particle diameter d_1 to d_2 is calculated by dividing the integrated particle formation rate at d_2 by the integrated particle formation rate at d_1, i.e.,

$$P_{d_1-d_2} = \frac{\int_{t_1}^{t_2} J_{d_2} dt}{\int_{t_1}^{t_2} J_{d_1} dt} \quad \text{(S2)}$$

where t_1 and t_2 are the lower and upper limits for integration, J_{d_1} and J_{d_2} are calculated by Eq. S1 at $d_{min} = d_1$ and $d_{min} = d_2$, respectively. In the calculation of $P_{d_1-d_2}$, particles of size d_1 formed at a specific time is not traced as they grow; instead, $P_{d_1-d_2}$ is an event-averaged particle survival probability for all particles that grow from d_1 to d_2. Since Eq. S2 is based on Eq. S1, it does not account for primary particle emissions, either.

S2. The 5+ simulations

We have conducted simulations in which only the evolution of $\geq$ 5 nm particles are simulated (hence termed '5+ simulations'). In these simulations, the sub 5 nm particle size distributions in the simulation are taken from the measured distribution, with the growth of ~ 5 nm particles and the coagulation of sub 5 nm particles serving as particle sources for the simulations above 5 nm. The cluster dynamics module still runs as a source of the SA_xDMA_y clusters whose condensation contributes to particle growth. However, the particles (containing more than 4 SA molecules) produced by the cluster dynamics module are lost rather than going into the sections. The time-resolved compositions of the ~5 nm particles, which affect the particle growth rate but are not available from the field observations, are taken from the corresponding full simulations.

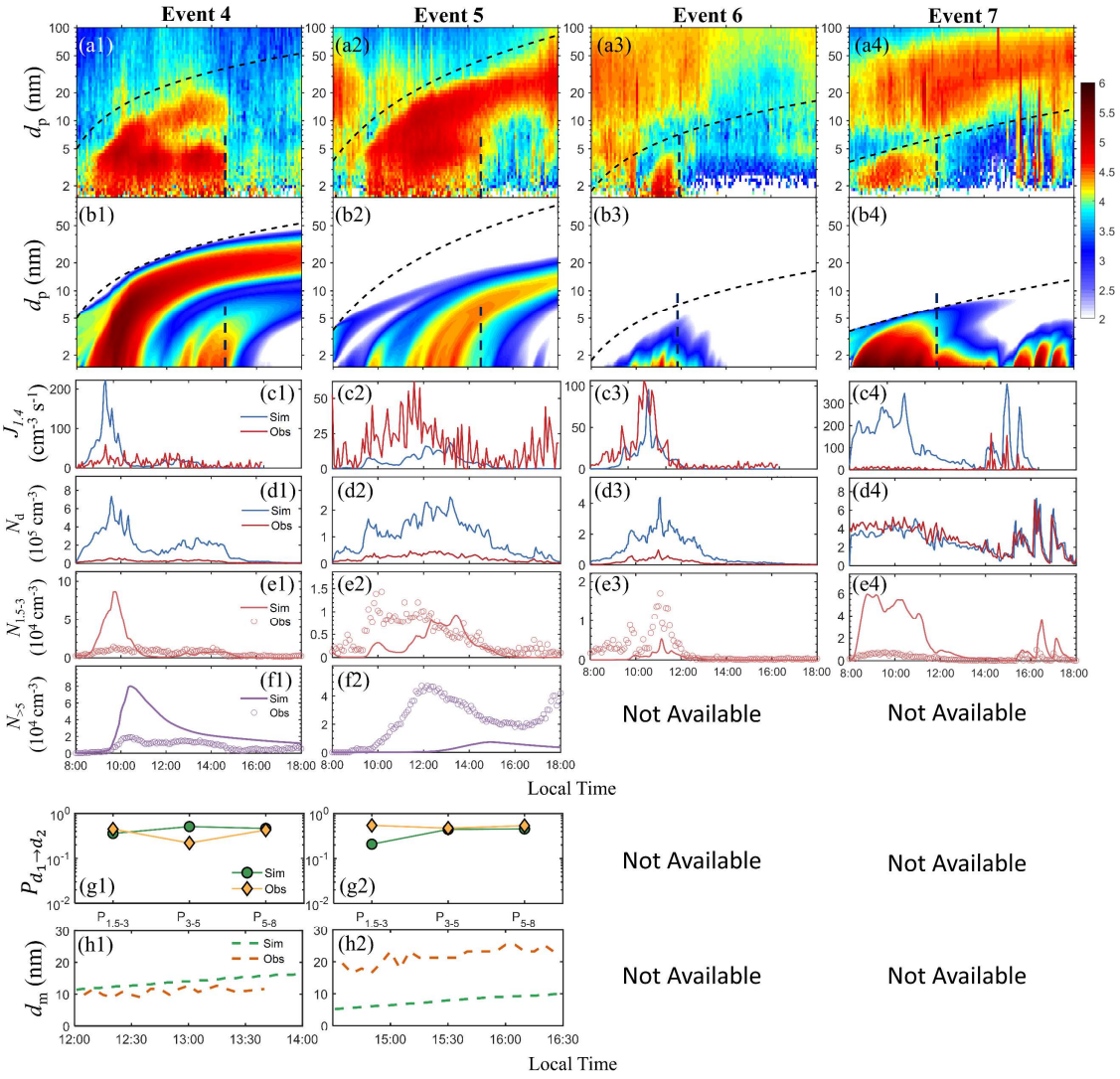

Figure S1. Comparison between the observation and the base case simulation for events 4-7. (a) The observed particle size distribution. (b) The simulated particle size distribution. In (a) and (b), the black dashed curves are reference curves that enclose the upper boundary of the observed PSDs which appear to originate from NPF. Vertical dashed lines approximately mark the end of the observed NPF events. (c) The simulated and the observed NPF rates at an electrical mobility diameter of 1.4 nm. (d) The simulated and the observed SA dimer concentration. (e), (f) The simulated and observed particle number concentrations between 1.5-3 nm and between 5 nm and the reference curves. (g) The simulated and the observed particle survival probability from 1.5 nm to 3 nm, from 3 nm to 5 nm and from 5 nm to 8 nm. (**h**) The simulated and the observed mode diameters during 12:00-14:00 (event 4) and during 14:30 and 16:30 (event 5).

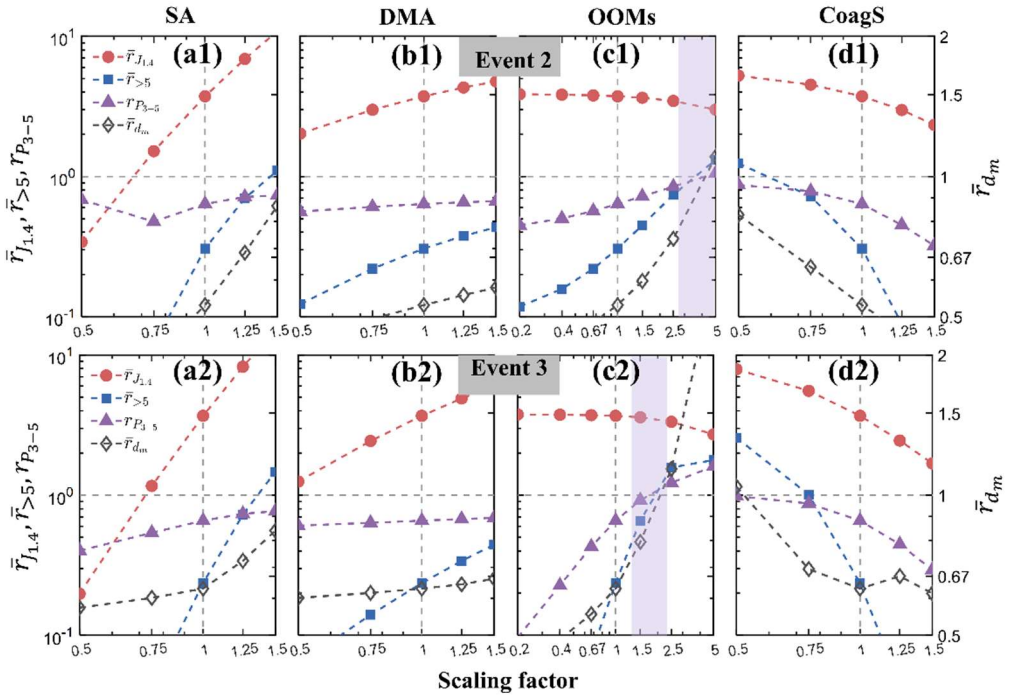

Figure S2. The sensitivity of $\bar{r}_{J_{1.4}}$, $\bar{r}_{>5}$, $r_{P_{3-5}}$ and $\bar{r}_{d_m}$ (see Table 2 for explanations of these quantities) to SA, DMA and OOMs concentrations and CoagS for event 2 (first row) and event 3 (second row). In the calculation, $\bar{r}_{J_{1.4}}$, $\bar{r}_{>5}$ were calculated with values averaged from 8:00 to 18:00, while $\bar{r}_{d_m}$ was calculated with values averaged between 14:30 and 16:30. $\bar{r}_{J_{1.4}}$, $\bar{r}_{>5}$ and $r_{P_{3-5}}$ correspond the left y-axis, and $\bar{r}_{d_m}$ corresponds to the right y-axis. Two reference lines are shown in each plot to aid visualization: the horizontal dashed line corresponds to a ratio of unity, while the vertical dashed line corresponds to the base simulation condition. The purple shaded areas cover OOMs scaling factors at which $\bar{r}_{>5}$, $r_{P_{3-5}}$ and $\bar{r}_{d_m}$ converge to unity.

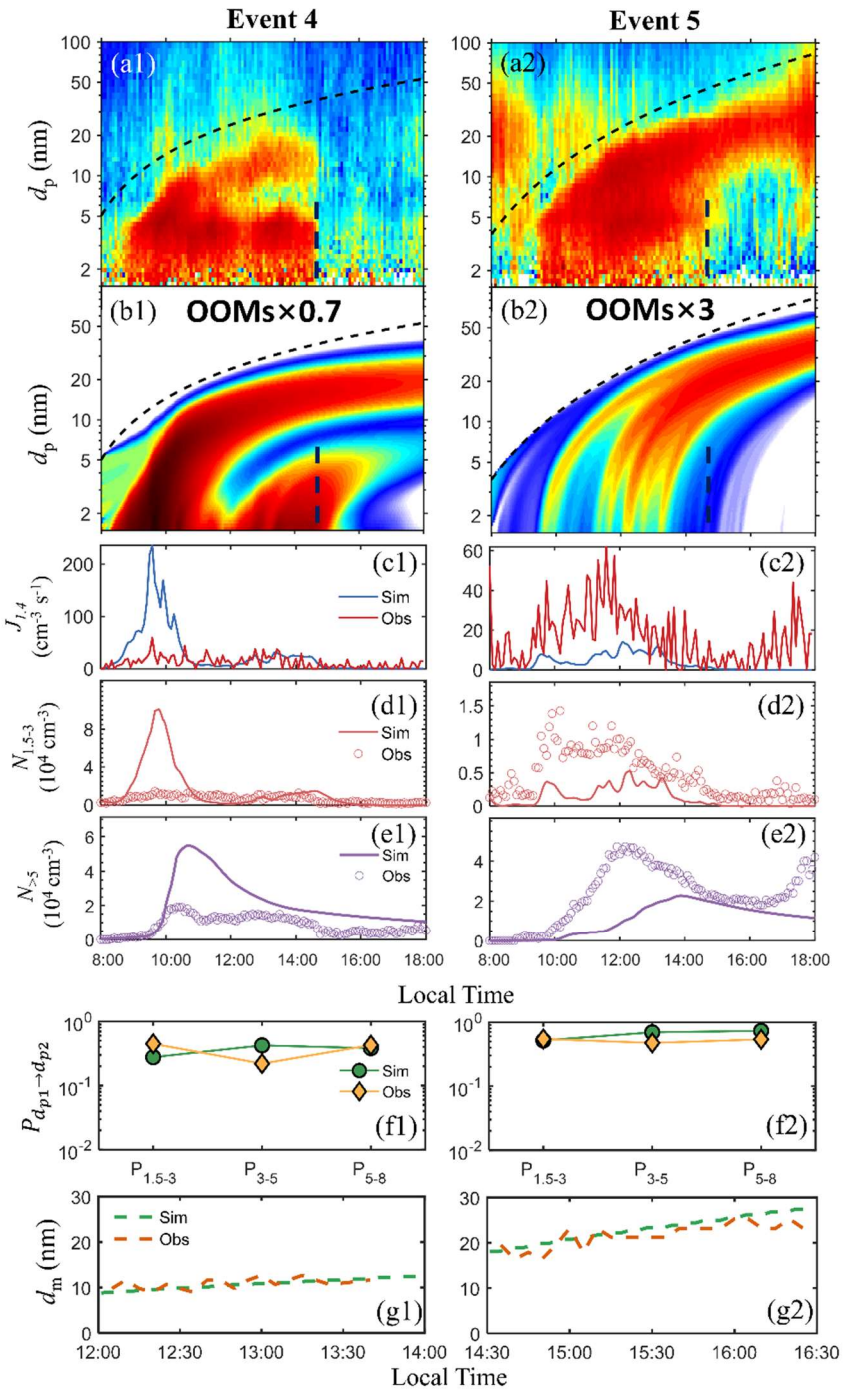

Figure S3. Comparison between the observation and the improved simulation for events 4 and 5. (a) The observed particle size distribution. (b) The simulated particle size distribution. In (a) and (b), the black dashed curves are reference curves that enclose the upper boundary of the observed PSDs which appear to originate from NPF. Vertical dashed lines approximately mark the end of the observed NPF events. (c) The simulated and the observed NPF rates at an electrical mobility diameter of 1.4 nm. (d) The simulated and the observed SA dimer concentration. (e), (f) The simulated and observed particle number concentrations between 1.5-3 nm and between 5 nm and the reference curves. (g) The simulated and the observed particle survival probability from 1.5 nm to 3 nm, from 3 nm to 5 nm and from 5 nm to 8 nm. (h) The simulated and the observed mode diameters during 12:00-14:00 (event 4) and during 14:30 and 16:30 (event 5).

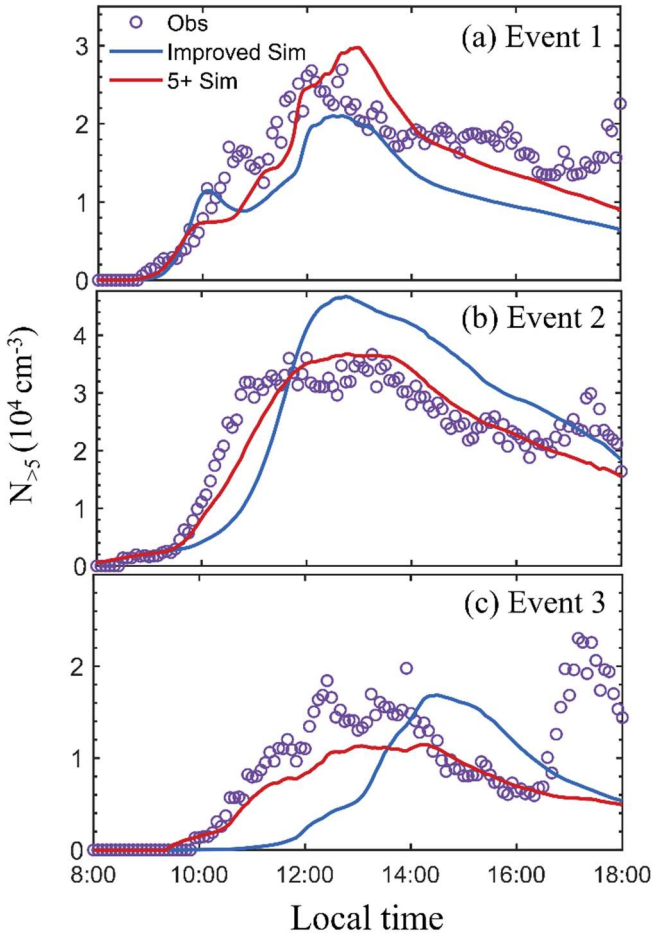

Figure S4. A comparison of $N_{>5}$ from the field observation, the improved simulations, and the 5+ simulations for events 1-3.

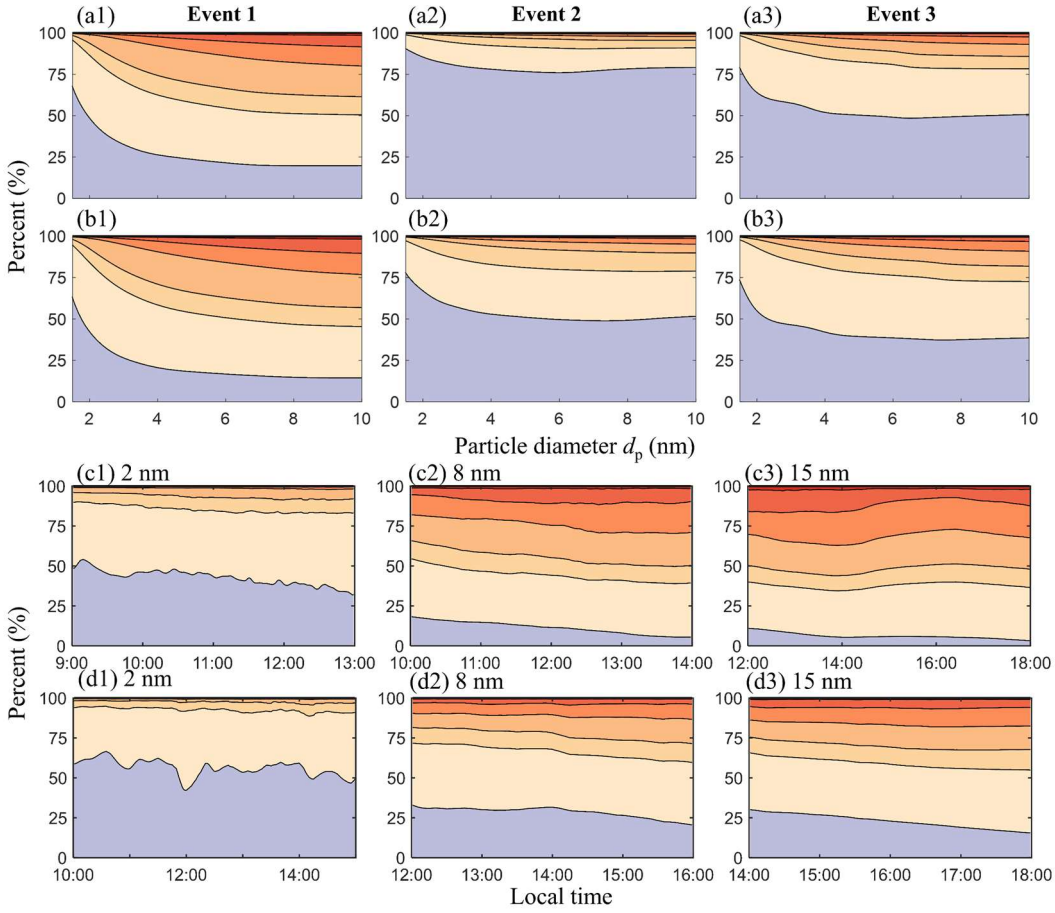

Figure S5. (a), (b) Composition of the particles smaller than 10 nm at 11:00 for events 1-3. (a) and (b) correspond to the base simulation and the improved simulations, respectively. (c), (d) Particle composition variation with time at fixed particle sizes (2 nm, 8 nm and 15 nm) for event 1 (row c) and event 3 (row d) in the improved simulations.

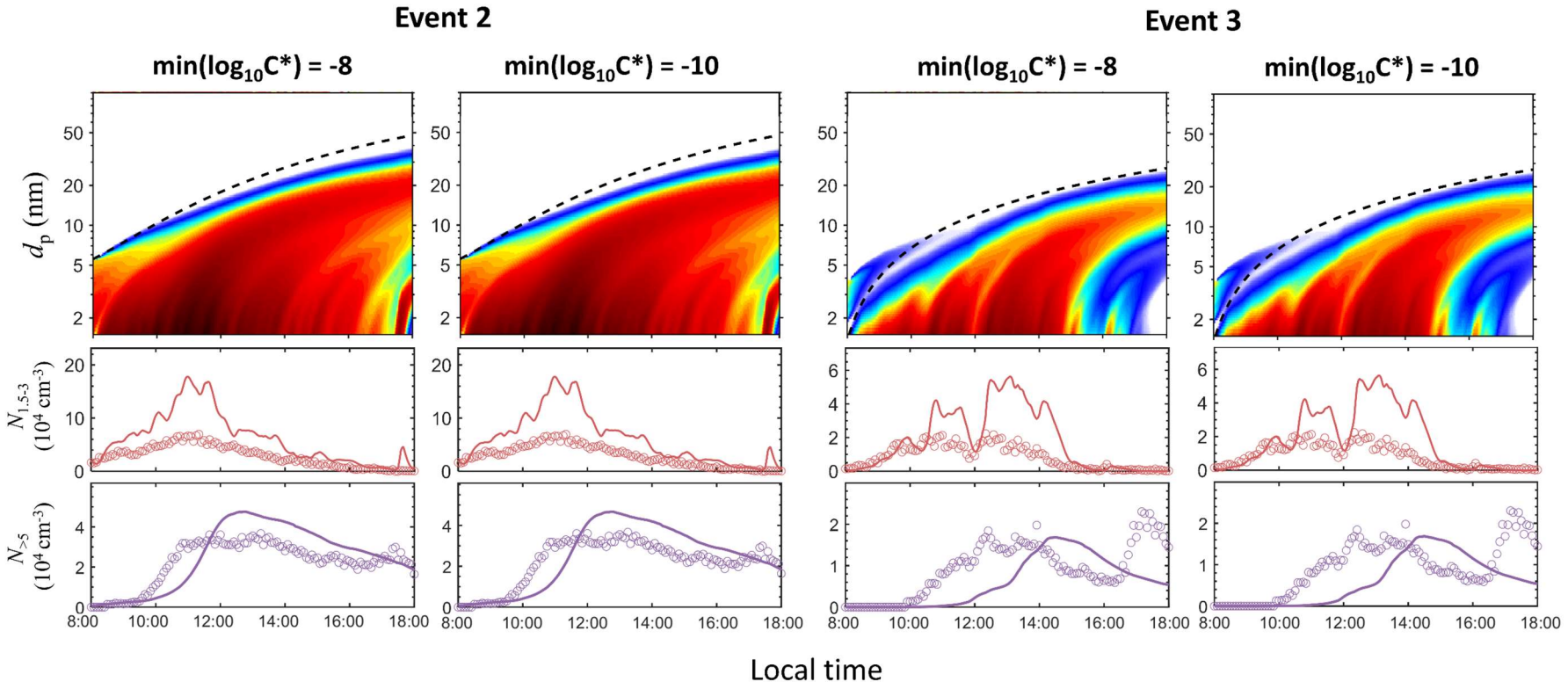

Figure S6. Comparison of the simulation results with 9 ($log_{10}C^*$ = -8-0) and 11 ($log_{10}C^*$= -10-0) volatility bins for OOMs at the conditions of the improved simulations for event 2 and event 3. Identical results are produced by the simulation with 9 and 11 bins, indicating that using 10 volatility bins with $log_{10}C^*$ = -8-0 are sufficient for accurately simulating particle condensation growth.